Available online at www.sciencedirect.com

SCIENCE DIRECT®

International Journal of Mass Spectrometry 232 (2004) 147–150

International Journal of Mass Spectrometry

www.elsevier.com/locate/ijms

Short communication

Dissociative electron impact ionization of N_2O_5

A. Abedi[1], P. Cicman[2], B. Coupier[3], B. Gulejová[2], G.A. Buchanan[4], G. Marston[4], N.J. Mason[5], P. Scheier, T.D. Märk*

Institut für Ionphysik, Leopold-Franzens Universität Innsbruck, Technikerstrasse 25, 6020 Innsbruck, Austria

Received 22 August 2003; accepted 8 December 2003

Abstract

Electron impact ionization of dinitrogen pentoxide for incident electron energies up to about 25 eV has been investigated by use of a crossed beams quadrupole mass spectrometer system. The experiments reported in this paper detected the fragmentation products NO_2^+, NO^+, O^+, N^+, and NO_3^+. No stable $N_2O_5^+$ ion was observed. The NO_3^+ fragment, for which we determine an appearance energy 13.25 ± 0.30 eV, has not been observed previously. This appearance energy is close to the calculated threshold.

Keywords: Appearance energy; Dinitrogen pentoxide; Electron ionization; Mass spectrometry

1. Introduction

Dinitrogen pentoxide, N_2O_5, plays a prominent role in the chemistry of both the Earth's troposphere and stratosphere. In the stratosphere, it is a reservoir molecule for the nitrogen oxides, NO_x, which are intricately involved in stratospheric ozone depletion. In the troposphere, its hydrolysis leads the formation of nitric acid (a major component of acid rain) and it exists in equilibrium with NO_3, the major nighttime oxidant [1]. It has also been implicated in the release of Cl atoms from sea-salt aerosol, reaction with NaCl giving the photolabile species $ClNO_2$ [2]. Despite of its current atmospheric importance [3–5] there have been only a few studies of its ionization properties. These studies include: the measurement of a He I photoelectron spectrum [6]; a photoionization study at photon energies between 10 and 20 eV reporting appearance energies for O^+, NO^+ and NO_2^+ fragment ions [7] and an early electron impact study reporting the production of NO^+ and NO_2^+ fragment ions at a nominal electron energy of 11.5 eV [8]. Most recently Price and coworkers reported relative partial ionization cross sections for N^+, O^+, NO^+ and NO_2^+ at energies in excess of 30 eV [9] and measured coincidence spectra of product dinitrogen pentoxide dications to derive the appearance energies for forming the $NO^+ + NO_2^+$ and $O^+ + NO^+$ ion pairs [10].

This lack of data can be partially explained by the difficulty in preparing pure samples of N_2O_5 and its reactivity in the mass spectrometer inlet system. Obviously, for reactive molecules it is no easy task to record a reproducible mass spectrum, in particular due to the tendency of reactive species to decompose on contact with many metallic or certain non-metallic surfaces [11]. Using our high resolution electron impact crossed molecular beams apparatus [12] and taking considerable care to prepare uncontaminated N_2O_5 samples and after taking into account any possible decomposition pathways we have measured the appearance energies of the various fragment ions produced in electron impact of N_2O_5. In addition, we were able to detect for the first time the production of the fragment ion NO_3^+ and to measure its appearance energy.

---

* Corresponding author. Adjunct professor: Department of Plasmaphysics, University Bratislava, Bratislava SK-84248, Slovak Republic.

E-mail address: Tilmann.Maerk@uibk.ac.at (T.D. Märk).

[1] Permanent address: Chemistry Department, Isfahan University of Technology, Isfahan 84154, Iran.

[2] Permanent address: Department of Plasmaphysics, University Bratislava, Bratislava SK-84248, Slovak Republic.

[3] Permanent address: Institut de Physique Nucléaire de Lyon, IN2P3-CNRS et Université Lyon I 43 boulevard du 11 Novembre 1918, F-69622 Villeurbanne Cedex, France.

[4] Permanent address: School of Chemistry, University of Reading, Whiteknights RG6 AD, United Kingdom.

[5] Permanent address: Department of Physics and Astronomy, The Open University, Walton Hall, Milton Keynes MK7 6AA, United Kingdom.

1387-3806/$ – see front matter © 2003 Elsevier B.V. All rights reserved.
doi:10.1016/j.ijms.2003.12.006

2. Experimental

The experiments were performed with a crossed electron/molecular beams apparatus that has been described previously in detail [12]; hence, only a few salient features are given here. The electron beam is produced using a custom-built trochoidal electron monochromator (TEM) [13], which is capable of achieving an energy resolution of about 35 meV under optimum conditions, albeit at rather low electron current of about 1 nA. In this work the instrument was operated at an electron resolution of about 100–200 meV (measured as full width at half maximum, FWHM) allowing operation of the monochromator at much higher electron currents of about 50 nA. The electron beam crossed the molecular beam (formed by an unreactive glass capillary) perpendicularly. The ions formed in the interaction region were extracted by a weak electric field into the entrance of a quadrupole mass spectrometer. The mass-selected positive ions were detected by a channeltron and the pulses were processed employing a pulse-counting technique and stored in a computer. The intensity of the mass-selected positive ion current was recorded as a function of the electron acceleration voltage. In order to obtain values for the appearance energies from the raw data, a fitting procedure was used [14,15], where the fitting function $F(E)$ was chosen based on Wannier's law. With this procedure, both the Wannier exponents p and the appearance energies AE can be extracted from the experiment; for further details on this technique, see [16]. Depending on the fragment ion under study we had to use either a fitting function with one ionization threshold or a fitting function with two ionization thresholds (i.e., corresponding to a situation in which an additional break in the ionization curve indicates the occurrence of an additional production channel at this 'second' ionization energy). The electron energy scale was calibrated using the same fitting procedure on electron impact ionization data of Ar using the known threshold of Ar as 15.759 ± 0.001 eV [17].

In the present experiments the N_2O_5 sample was generated by the reaction of ozone and nitric oxide at ambient temperature [18], which can be represented stoichiometrically by the reaction

$$2NO + O_3 \rightarrow N_2O_5 \qquad (1)$$

The flow apparatus used in these experiments was made from glass and a series of Teflon taps to control the flow of the gases. Because N_2O_5 reacts readily with H_2O to form nitric acid, precautions were taken to ensure the system was dry. The flow system was evacuated overnight and dried thoroughly before introducing NO into the system, via a needle valve, through a trap that is held in an acetone/solid CO_2 slush bath at 195 K. NO was chosen as the precursor over NO_2 as it is easier to dry. O_3 is produced by flowing pure O_2 through a commercial ozonizer (Fischer 502) at a flow rate of about 100 l of O_2 per hour, producing about 5 g of O_3 per hour. The flows of NO and O_3 are merged at a controlled point in the glass manifold where NO is oxidised first to NO_2 and then to NO_3 which reacts with NO_2 to form N_2O_5. As the resulting product can be potentially contaminated with traces of unreacted NO_x, the flow rates of the feed gases are carefully adjusted so that there was no trace of NO_2 (a brown gas) after the desired point of reaction. The product was then collected for approximately 1 h in a cold trap held at 195 K. N_2O_5 is a white solid crystal with a melting point of 293 K and can be stored below 270 K for long time periods without deterioration. In order to avoid (minimize) decomposition of N_2O_5 (e.g., by reacting with metallic surfaces), we used glass tubes for the gas inlet to the TEM.

3. Results and discussion

Fig. 1 shows as an example a 70 eV electron impact ionization mass spectrum of N_2O_5 accompanied by traces of the calibration gas Ar. As reported in the previous studies we can see ions at $m/z = 14$ (N^+), $m/z = 16$ (O^+), $m/z = 30$ (NO^+) and $m/z = 46$ ($NO_2{}^+$) which can be ascribed to dissociative ionization of N_2O_5. Nevertheless, these ions could also be due to ionization of impurities in the sample cell (note the signals at $m/z = 28$ and 32 arising from nitrogen and oxygen impurities) or from decomposition products of N_2O_5 (see below). In contrast to earlier studies we have however also observed a signal at $m/z = 62$ which can be ascribed to the production of $NO_3{}^+$ from N_2O_5. The ion intensities observed here are, in descending order, $NO_2{}^+$, NO^+, O^+ and N^+, and are similar to the ratios observed by Price and co-workers [9]. The ion signal of $NO_3{}^+$ is an order of magnitude lower than any of the others and this low abundance may be the reason that this ion was not seen in the previous studies. As already reported in the previous studies, no stable parent ion $N_2O_5{}^+$ could be observed via ionization of N_2O_5.

$NO_2{}^+$: The ion yield curve near threshold of the $NO_2{}^+$ is shown in Fig. 2. A detailed analysis of this curve using the above described fitting procedure reveals that this curve has an onset at 9.90 eV and shows a break at 12.20 eV. The

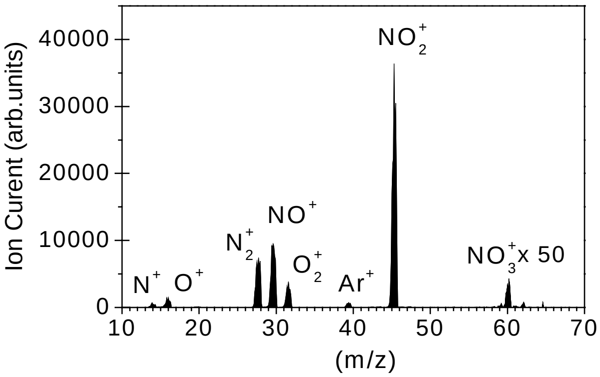

Fig. 1. Positive mass spectra of N_2O_5 mixed with a trace of Ar calibration gas.

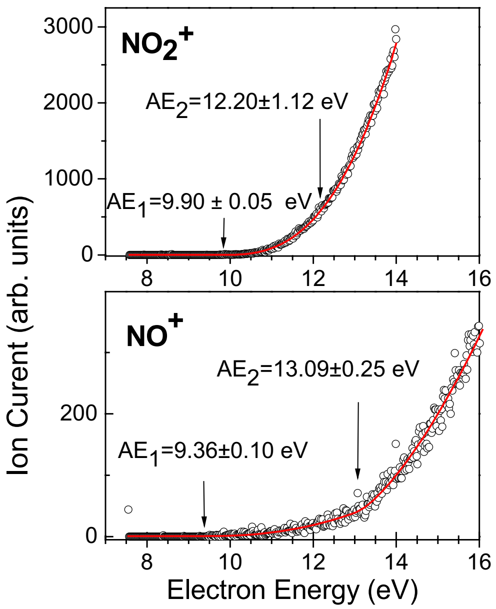

Fig. 2. Ion yield curve of NO_2^+ (upper panel) and of NO^+ (lower panel) for electron impact ionization of N_2O_5: circles experimental data points, full line: fit through the data points as described in text in order to deduce appearance energies.

formation of NO_2^+ by electron impact ionization of N_2O_5 is expected to occur according to the following reactions using thermo-chemical data from [19,20].

$$N_2O_5 + e \rightarrow NO_2^+ + NO_3 + 2e, \quad AE = 10.56\,eV \quad (2a)$$

$$N_2O_5 + e \rightarrow NO_2^+ + NO_2 + O + 2e, \quad AE = 12.75\,eV \quad (2b)$$

Thus, the first onset observed here at 9.90 ± 0.05 eV (the present error bars pertaining to the statistical error obtained from the fitting procedure) has to be attributed to the appearance of NO_2^+ via ionisation of NO_2 (the corresponding ionisation energy being 9.75 eV) being present in the sample (either as an initial impurity or as a decomposition product of N_2O_5). The second onset (break of the curve) at 12.20±1.12 eV agrees well with the photoelectron spectrum for N_2O_5 reported by Ames and Turner [6] which shows the lowest adiabatic ionisation energy at 11.4 eV and the corresponding vertical value at 12.3 eV. The photoionization yield curve of Jochims et al. [7] gave also a smooth onset in this energy region. It has therefore to be concluded that approximately 1.6 eV excess energy is involved in the NO_2^+ formation at threshold (part of it due to the difference between adiabatic and vertical threshold), but it should be taken into consideration that the accuracy of the thermochemical data used may not be very high.

NO^+: The ion yield curve near threshold of NO^+ is shown in Fig. 2. This curve also appears to show, according to our fitting analysis, more than one threshold with a first onset at 9.36 ± 0.10 eV and a second one at 13.09 ± 0.25 eV. As in the case of NO_2^+ the first onset can be attributed to the production of NO^+ via ionisation of NO being present in the sample (either as initial impurity or as a decomposition product of NO_2; the corresponding ionisation energy of NO being 9.26 eV). The second onset at 13.09 ± 0.25 eV is in excellent agreement with the earlier photoionization result of Jochims et al. [7] at 12.95 and very likely corresponds to the production of the NO^+ ion via one of the following reactions, one of them involving a considerable amount of excess energy, the other one being barely energetically possible.

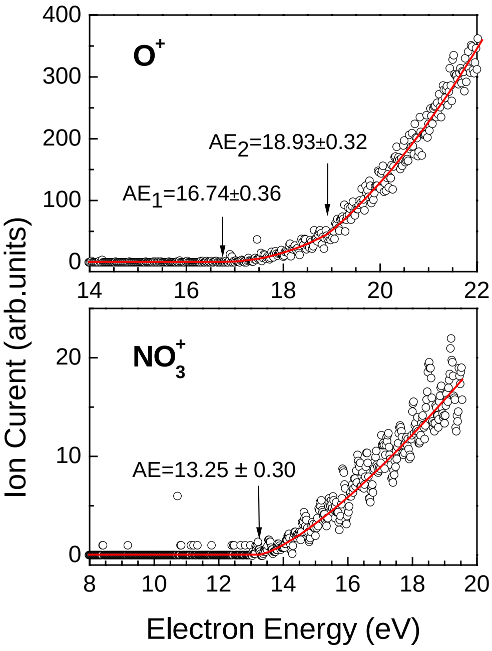

Fig. 3. Ion yield curve of O^+ (upper panel) and of NO_3^+ (lower panel) for electron impact ionization of N_2O_5: circles experimental data points, full line: fit through the data points as described in text in order to deduce appearance energies.

$$N_2O_5 + e \rightarrow NO^+ + NO_2 + O_2 + 2e, \quad AE = 10.45\,eV \quad (3a)$$

$$N_2O_5 + e \rightarrow NO^+ + NO_3 + O + 2e, \quad AE = 13.40\,eV \quad (3b)$$

O^+: The O^+ ion yield curve shows near threshold according to our fitting analysis an onset at 16.74 ± 0.36 eV and a break at 18.93 ± 0.32 eV (see Fig. 3). This result is in accordance with the photoionization results of Jochims et al. [7] reporting a weak O^+ ion yield with an onset between 16 and 17 eV. Possible production channels of O^+ from N_2O_5 include

$$N_2O_5 + e \rightarrow O^+ + N_2O_4 + 2e, \quad AE = 16.18\,eV \quad (4a)$$

$$N_2O_5 + e \rightarrow O^+ + 2NO_2 + 2e, \quad AE = 16.76\,eV \quad (4b)$$

$$N_2O_5 + e \rightarrow O^+ + NO + NO_3 + 2e, \quad AE = 17.73\,eV \quad (4c)$$

Whereas the first onset may be ascribed to reactions (4a or 4b) (or due to production of O^+ via ionisation of NO_2 present in the sample, see above; the corresponding ionization energy being 16.8 eV), the second onset could be due to production of O^+ via ionisation of O_2 present in the sample (either as initial impurity or as a decomposition product; the corresponding ionisation energy being 18.7 eV). It is interesting to note that Jochims et al. [7] also see a break at about this energy.

NO_3^+: The most important observation in the present work is the presence of the fragment ion NO_3^+ produced via electron impact ionization of N_2O_5. This ion has a rather low signal in comparison with the signal of other ions and this is the most likely the reason why it has not been observed in previous experiments. The ion yield curve near threshold of NO_3^+ is shown in Fig. 3 lower panel exhibiting an onset value of 13.25 ± 0.30 eV. On energetic reasons there is only the reaction

$$N_2O_5 + e \rightarrow NO_3^+ + NO_2 + 2e, \qquad AE = 13.53\,\text{eV} \qquad (5)$$

which may contribute to the production of this ion via ionisation of N_2O_5 at threshold and the calculated appearance energy is in good agreement with the measured value taking into account the involved error bars of the thermo-chemical data and the present determination. Moreover, it is interesting to note that the adiabatic ionization energy for the nitrate radical NO_3 as determined to be 12.57 ± 0.03 eV by Monks et al. [21] using a discharge flow-photoionization mass spectrometer apparatus coupled to a synchrotron radiation source is well below the present appearance energy, thus excluding contamination of the N_2O_5 target with the nitrate radical. It should be noted that the structure and the atmospheric implications of the existence of the NO_3^+ cation has been extensively studied and discussed recently [22].

Acknowledgements

This work was partially supported by the FWF and ÖNB, Vienna, Austria and by the EU Commission, Brussels as part of the FPV Network 'EPIC'. GAB thanks NERC, UK for a studentship.

References

[1] B.A. Thrush, Rep. Prog. Phys. 51 (1988) 1341.
[2] R.C. Hoffman, M.E. Gebel, B.S. Fox, B.J. Finlayson-Pitts, Phys. Chem. Chem. Phys. 5 (2003) 1780.
[3] C.A. Cantrell, J.A. Davidson, R.E. Shetter, B.A. Anderson, J.G. Calvert, J. Phys. Chem. 91 (1987) 6017.
[4] C.A. Cantrell, R.E. Shetter, J.G. Calvert, G.S. Tyndall, J.J. Orlando, J. Phys. Chem. 97 (1993) 9141.
[5] H. Wincel, E. Mereand, A.W. Castleman Jr., J. Phys. Chem. 99 (1995) 1792.
[6] D.L. Ames, D.W. Turner, Proc. R. Soc. Lond. A. 348 (1976) 175.
[7] H.W. Jochims, W. Denzer, H. Baumgärtel, O. Lösking, H. Willner, Ber. Bunsenges. Phys. Chem. 96 (1992) 573.
[8] G. Liuti, S. Dondes, P. Harteck, J. Phys. Chem. 72 (1968) 1081.
[9] C.S.S. O'Connor, N.C. Jones, K. O'Neale, S.D. Price, Int. J. Mass. Spectrom. Ion Proc. 154 (1996) 203.
[10] C.S.S. O'Connor, N.C. Jones, S.D. Price, Chem. Phys. 214 (1997) 131.
[11] K.A. Newson, S.M. Luc, S.D. Price, N.J. Mason, Int. J. Mass Spectrom. Ion Proc. 148 (1995) 203.
[12] V. Grill, H. Drexel, W. Sailer, M. Lezius, T.D. Märk, Int. J. Mass Spectrom. 205 (2001) 209.
[13] A. Stamatovic, G. Schulz, Rev. Sci. Instr. 39 (1968) 1752.
[14] S. Matt, O. Echt, R. Wörgötter, V. Grill, P. Scheier, C. Lifshitz, T.D. Märk, Chem. Phys. Lett. 264 (1997) 149.
[15] T. Fiegele, G. Hanel, I. Torres, M. Lezius, T.D. Märk, J. Phys. B: At. Mol. Opt. Phys. 33 (2000) 4263.
[16] M. Stano, S. Matejcik, J.D. Skalny, T.D. Märk, J. Phys. B: At. Mol. Opt. Phys. 36 (2003) 261.
[17] NIST Chemistry WebBook, http://webbook.nist.gov.
[18] J.A. Davidson, A.A. Viggiano, C.J. Howard, I. Dotan, F.C. Fehsenfeld, D.L. Albritton, E.E. Ferguson, J. Chem. Phys. 68 (1978) 2085.
[19] D.R. Lide (Ed.), Handbook of Chemistry and Physics, 1992, p. 10.
[20] M.W. Chase Jr., J. Phys. Chem. Ref. Data 9 (1998) 1.
[21] P.S. Monks, L.J. Stief, M. Krauss, S.C. Kuo, Z. Zhang, R.B. Klemm, J. Phys. Chem. 98 (1994) 10017.
[22] F. Cacace, G. de Petris, M. Rosi, A. Troiani, Chem. Eur. J. 8 (2002) 5684.